Published in final edited form as:

AJR Am J Roentgenol. 2013 November ; 201(5): 1041–1048. doi:10.2214/AJR.13.10591.

Prostate Volumes Derived From MRI and Volume-Adjusted Serum Prostate-Specific Antigen: Correlation With Gleason Score of Prostate Cancer

Ibrahim Karademir[1], **Dinggang Shen**[2], **Yahui Peng**[1], **Shu Liao**[2], **Yulei Jiang**[1], **Ambereen Yousuf**[1], **Gregory Karczmar**[1], **Steffen Sammet**[1], **Shiyang Wang**[1], **Milica Medved**[1], **Tatjana Antic**[3], **Scott Eggener**[4], and **Aytekin Oto**[1]

[1]Department of Radiology, University of Chicago, 5841 S Maryland Ave, MC 2026, Chicago, IL 60637

[2]Department of Radiology, University of North Carolina, Chapel Hill, NC

[3]Department of Pathology, University of Chicago, Chicago, IL

[4]Department of Surgery, Section of Urology, University of Chicago, Chicago, IL

Abstract

OBJECTIVE—The purpose of this article is to study relationships between MRI-based prostate volume and volume-adjusted serum prostate-specific antigen (PSA) concentration estimates and prostate cancer Gleason score.

MATERIALS AND METHODS—The study included 61 patients with prostate cancer (average age, 63.3 years; range 52–75 years) who underwent MRI before prostatectomy. A semiautomated and MRI-based technique was used to estimate total and central gland prostate volumes, central gland volume fraction (central gland volume divided by total prostate volume), PSA density (PSAD; PSA divided by total prostate volume), and PSAD for the central gland (PSA divided by central gland volume). These MRI-based volume and volume-adjusted PSA estimates were compared with prostatectomy specimen weight and Gleason score by using Pearson (r) or Spearman (ρ) correlation coefficients.

RESULTS—The estimated total prostate volume showed a high correlation with reference standard volume ($r = 0.94$). Of the 61 patients, eight (13.1%) had a Gleason score of 6, 40 (65.6%) had a Gleason score of 7, seven (11.5%) had a Gleason score of 8, and six (9.8%) had a Gleason score of 9 for prostate cancer. The Gleason score was significantly correlated with central gland volume fraction ($\rho = -0.42$; $p = 0.0007$), PSAD ($\rho = 0.46$; $p = 0.0002$), and PSAD for the central gland ($\rho = 0.55$; $p = 0.00001$).

CONCLUSION—Central gland volume fraction, PSAD, and PSAD for the central gland estimated from MRI examinations show a modest but significant correlation with Gleason score and have the potential to contribute to personalized risk assessment for significant prostate cancer.

Address correspondence to A. Oto (aoto@radiology.bsd.uchicago.edu).

Keywords

Gleason score; MRI; prostate cancer

Prostate cancer is a heterogeneous disease that ranges clinically from indolent to highly aggressive. It is estimated that one in six American men will be diagnosed with prostate cancer in their lifetime, but only a small proportion of these patients will die of the disease. Various methods for prostate cancer risk assessment (e.g., nomograms) have been devised that incorporate laboratory findings (e.g., serum prostate-specific antigen [PSA] concentration), patient demographics (e.g., age), and clinical findings (e.g., digital rectal examination) to differentiate intermediate-and high-risk patients (i.e., those who benefit from aggressive therapy such as radical prostatectomy and radiation therapy) from low-risk patients (i.e., those who benefit from active surveillance) [1–5]. However, despite these methods, overtreatment of prostate cancer remains an important clinical issue, and there is a need for better and personalized risk assessment at the time of diagnosis [6, 7]. Overtreatment of prostate cancer leads to serious complications (such as impotence and incontinence) that affect the quality of life of the patients, and it unnecessarily increases healthcare costs.

Current knowledge of the anatomic structure of the prostate is largely based on the clinically significant zonal classification of McNeal [8]. Typically, the transition zone (TZ) is the site of benign prostatic hyperplasia (BPH), whereas peripheral zone (PZ) cancer accounts for 75–85% of all prostate cancer cases [9]. Furthermore, compared with PZ cancer, TZ cancers often have a more favorable prognosis, with a lower Gleason score, less frequent extracapsular extension and seminal vesicle invasion, and a lower rate of biochemical recurrence [10–13]. Given these differences in cancer risk and cancer aggressiveness between the TZ and PZ, we hypothesize that prostate zonal volume information can be useful in the assessment of personalized risk of aggressive prostate cancer. In addition, serum PSA values adjusted by prostate zonal volume have the potential to improve prostate cancer diagnosis and reduce unnecessary biopsies.

MRI can be used to visually differentiate the PZ from the central gland—that is, the combination of the TZ and the central zone [14–19]. In patients 50 years old and older, the TZ typically enlarges because of BPH and comprises most of the central gland. MRI may also be more accurate than transrectal ultrasound and CT for prostate volume estimation [20–25]. Superior contrast resolution of MRI compared with transrectal ultrasound may also lead to the possibility of application of tumor volume–adjusted PSA levels for the assessment of prostate cancer aggressiveness. The purpose of this study was to study relationships between MRI-based prostate volume and volume-adjusted serum PSA concentration estimates (in terms of both total and zonal volumes) and Gleason score.

Materials and Methods

Patients

This retrospective study was conducted with an institutional review board–approved waiver of informed consent and was in compliance with the HIPAA. We searched patient records at our institution to identify 65 consecutive patients diagnosed with prostate cancer between September 2008 and February 2010 who underwent multiparametric endorectal MRI on 1.5-T scanners, subsequently underwent radical prostatectomy, and did not receive radiation or hormonal therapy before MRI. We excluded four patients because of missing prostatectomy specimen weight data. Thus, 61 patients were included in this study: the median age was 64 years (average, 63.3 years; range, 52–75 years), and the median PSA level was 6.1 ng/mL (average, 10.2 ng/mL; range, 0.8–65 ng/mL).

MRI Protocols

All MRI scans were done with both an endorectal coil (Prostate eCoil, Medrad) and a phased-array surface coil in one of two 1.5-T MRI scanners (Achieva, Philips Healthcare [n = 31]; or Excite, GE Healthcare [n = 30]). Immediately before the MRI scan, 1 mg of glucagon was injected intramuscularly. We imaged the entire prostate and oriented axial images to be perpendicular to the rectal wall, guided by sagittal images. A parallel imaging factor of 2 was used in all sequences. The following images were obtained: axial, coronal, and sagittal T2-weighted fast spin-echo (for the Achieva scanner: TR/TE, 5000/120; matrix size, 204 × 256; echo-train length, 24; number of signals acquired, 4; section thickness, 3 mm; intersection gap, 0 mm; FOV, 14–18 cm; and spatial resolution, 0.8 × 0.8 × 3 mm; for the Excite scanner: TR/TE, 3200– 3500/90–100; matrix size, 192 × 256; echo-train length, 19; number of signals acquired, 4; section thickness, 3 mm; intersection gap, 0 mm; and FOV, 14–16 cm), axial T1-weighted fast spin-echo, axial free-breathing diffusion-weighted MRI, and axial free-breathing dynamic contrast-enhanced MRI (DCE-MRI). Acquisition of DCE-MRI examinations (of the entire prostate) started 30 seconds before IV bolus administration of 0.1 mmol/kg gadodiamide (Omniscan, GE Healthcare), which was followed immediately by a 20-mL saline flush at the rate of 2.0 mL/s. The total image acquisition time was approximately 45 minutes. Detailed acquisition protocols are given in Appendix 1.

MRI-Based Volume Estimation

Volume calculations of the whole prostate and central gland derived from T2-weighted MRI examinations were performed in a semiautomated fashion on the basis of the nonlocal mean sparse representation method developed in CT images [26]. Prostate volume estimation was based on computer segmentation of the entire prostate and the central gland from T2-weighted MRI examinations, a summary of which is provided in Appendix 1. A radiologist with 10 years' experience in prostate MRI reviewed computer outlines of the entire prostate and the central gland obtained for each MRI slice and manually corrected the computer image-segmentation results to ensure accuracy, especially at the base and the apex of the prostate. The ITK-SNAP software (Penn Image Computing and Science Laboratory) was adapted for this manual correction task. Subsequently, the same software was used to calculate automatically the total and central gland prostate volumes according to the

corrected computer outlines. The PZ volume was then calculated by subtracting the central gland volume from the total prostate volume. We define central gland volume fraction as the central gland volume divided by the total prostate volume.

Reference Standard of Prostate Volume

Total prostate weight was obtained from pathology reports. At our institution, surgically resected fresh prostatectomy specimens are weighed, and the weight is noted in the pathology report. A strong correlation between prostate weight and displaced water volume (correlation coefficient, 0.997) was reported previously [27, 28]. Rodriguez, Jr. et al. [27] showed that the average weight of seminal vesicles was 3.8 g, and, thus, we subtracted 3.8 g from the total specimen weight to estimate the total prostate weight without seminal vesicles for 57 of 61 (93.4%) patients whose prostate specimens were weighted together with seminal vesicles. For the other four patients, the prostate weight was available in the pathology report. We then divided the estimated total prostate weight by 1.05 g/ mL (density of prostatic tissue) and used the resulting volume estimate as the reference standard, as in earlier studies [29]. An identical reference standard for prostate volume was also described in a previously published study [25].

Gleason Scores

A genitourinary pathologist with 8 years' experience in prostate histology reviewed all histopathologic slides from the radical prostatectomy specimen and reassessed the Gleason score in each case. As in routine clinical practice, the pathologist assigned for the entire specimen a Gleason grade for the most common tumor pattern and a second Gleason grade for the next most common tumor pattern. Gleason score was the sum of these two Gleason grades.

Volume-Adjusted PSAs (PSA Densities)

Volume-adjusted PSA, or PSA density (PSAD), was calculated by dividing PSA concentration by the total prostate volume. Central gland volume-adjusted PSA (PSAD of central gland) was calculated by dividing PSA concentration by the central gland volume, and PZ volume-adjusted PSA (PSAD of PZ) was calculated by dividing PSA concentration by the PZ volume.

Statistical Analysis

The Pearson correlation coefficient (r) was calculated between the total prostate volume and the reference standard of prostate volume. A simple linear regression analysis was also performed between the reference standard of prostate volume and the estimated total prostate volume. Spearman correlation coefficient (ρ) was calculated between Gleason score and patient age, PSA, total prostate volume, PZ volume, central gland volume, central gland volume fraction, PSAD, PSAD of central gland, and PSAD of PZ. The effectiveness of central gland volume fraction, PSAD, and PSAD of central gland in differentiating between lowgrade (Gleason score < 7) and high-grade (Gleason score ≥ 7) prostate cancers was evaluated by using maximum likelihood–estimated proper-binormal receiver operating characteristic curves and the area under the receiver operating characteristic curve [30].

Sensitivity, specificity, positive predictive value, and negative predictive value, with an empirically selected threshold value, were also calculated for the three variables. All *p* values were two tailed. Statistical significance was considered at the level of *p* less than 0.05 for each individual correlation coefficient and also at the level of *p* less than 0.005 after Bonferroni correction for the 10 correlation coefficients that we calculated in this study. All statistical analysis was done with in-house computer software written in the Python scripting language (Python Software Foundation).

Results

Total and Zonal Prostate Volumes

An example of a computer-segmentation result on T2-weighted MRI examinations of the entire prostate and the central gland is shown in Figure 1. For the reference standard of prostate volume, the average total prostate volume was 50.44 cm^3 (SD, 19.3 cm^3; median, 49.3 cm^3; range, 20.2–131.8 cm^3). The estimated total, central gland, and PZ prostate volumes are summarized in Table 1. Correlation between estimated total prostate volume and the reference standard of prostate volume is shown in Figure 2 ($r = 0.94$; $p < 0.0001$). A simple linear regression between the reference standard of prostate volume and the estimated total prostate volume yielded a regression coefficient (slope) of 0.86. The estimated total prostate volume was, on average, approximately 4.0 cm^3 (or 10%) smaller than the reference standard of prostate volume (range, −18.0 cm^3 [−40%] to 10.0 cm^3 [20%]).

Correlation Between Gleason Score and Estimated Prostate Volumes

The Gleason score was 6 in eight (13.1%) patients, 7 in 40 (65.6%) patients, 8 in seven (11.5%) patients, and 9 in six (9.8%) patients. The median estimated total prostate volume was 55.4, 42.7, 47.3, and 34.0 cm^3, and the median estimated central gland volume was 34.8, 21.6, 20.3, and 17.2 cm^3 in patients with Gleason scores of 6, 7, 8, and 9, respectively. A modest significant negative correlation was found between Gleason score and the central gland volume fraction ($\rho = -0.42$; $p = 0.0007$), and a moderate borderline significant negative correlation was found between Gleason score and the estimated central gland volume ($\rho = -0.33$; $p = 0.01$), whereas the apparent correlation between Gleason score and the other parameters was not statistically significant. Box plots of the estimated central gland volume and central gland volume fraction stratified by Gleason score are shown in Figure 3. Spearman correlation coefficients between Gleason score and patient age, PSA, estimated total volume, PZ volume, and central gland prostate volume, and estimated central gland volume fraction are listed in Table 2.

Correlation Between Gleason Score and PSADs

Box plots of PSAD and PSAD of the central gland stratified by Gleason score are shown in Figure 4. The median PSAD was 0.10, 0.14, 0.26, and 0.31 ng/mL/cm^3, and the median PSAD of the central gland was 0.16, 0.27, 0.44, and 0.66 ng/mL/cm^3 in patients with Gleason scores of 6, 7, 8, and 9, respectively. Both PSAD ($\rho = 0.46$; $p = 0.0002$) and PSAD of the central gland ($\rho = 0.55$; $p = 0.00001$) were found to correlate significantly with Gleason score (Table 2). The area under the receiver operating characteristic curve values (±

standard error) for differentiating between prostate cancers with a Gleason score less than 7 versus a Gleason score of 7 or greater are 0.84 ± 0.05 for central gland volume fraction, 0.77 ± 0.07 for PSAD, and 0.84 ± 0.05 for PSAD of the central gland. Sensitivity, specificity, positive predictive value, and negative predictive value, based on an empirically selected threshold value, are shown in Table 3.

Discussion

Estimation of the total and TZ prostate volume has been used clinically for evaluation of BPH and for adjusting PSA level by prostate volume to help increase specificity for prostate cancer diagnosis [31–40]. Kaplan et al. [31] found that TZ volume is a better proxy of BPH size than the total prostate volume and described a TZ index (ratio of the TZ to total prostate volume) that they found correlates significantly with clinical parameters of BPH. In that study, the total or TZ prostate volumes were estimated under an assumed ellipsoid approximation of the prostate (volume = length × width × height × π / 6), with the three linear dimensions estimated from transrectal ultrasound.

The ellipsoid approximation assumption has inherent limitations. A hypertrophied prostate with an irregular contour does not satisfy this assumption [23]. Furthermore, because the prostate volume is calculated by multiplying three linear dimensions, a small error in one dimension can lead to a large and amplified error in the estimate of the total volume. In addition, transrectal ultrasound estimation of linear dimensions is known to vary in patients with large prostates and when observer experience varies [23].

MRI provides soft-tissue contrast resolution superior to that of transrectal ultrasound and CT and, therefore, can be used for more accurate estimation of prostate volume [20, 21]. Automated or semiautomated segmentation methods can be applied to prostate MRI examinations and allow accurate volume estimation with minimal interobserver variations [24, 25]. Our semiautomated MRI-based prostate segmentation method produced total prostate volume estimates that highly correlated with prostate weight (correlation coefficient, 0.94). MRI can also be used to delineate the central gland from the PZ [13–19] because of differences in T2 relaxation times and the presence of a pseudocapsule between them [17, 40]. On T2-weighted images, it may be even possible to distinguish different histologic types (e.g., stromal vs cystic hyperplasia) of BPH [14, 16]. It is possible to obtain all of these results in all clinical MRI studies of the prostate, to aid the diagnosis and follow-up assessment of patients with BPH and prostate cancer.

Our results showed a modest significant negative correlation between Gleason score and the central gland volume fraction. The correlation between estimated central gland volume and Gleason score was borderline significant. However, no statistically significant correlation was found between Gleason score and the total prostate volume or between Gleason score and the PZ volume. Previous studies of large populations and transrectal ultrasound– based volume estimates showed significantly decreased TZ volume in patients with prostate cancer compared with patients with BPH [34, 35, 38]. In a study by Ohi et al. [38], the TZ volume was smaller in patients with prostate cancer (9.5 vs 18.0 mL), whereas the total prostate volume was similar (27.2 mL vs 33.7 mL). Tanaka et al. [40] analyzed 235 patients with

intermediate PSA levels (4.1– 10 ng/mL) and found that the total prostate volume and the TZ volume had significantly greater predictive values for the diagnosis of prostate cancer compared with that of serum PSA. However, despite these promising findings on the relationship between prostate volumes and prostate cancer, issues of lack of reproducible and inaccurate volume estimates from transrectal ultrasound have limited widespread clinical use of volume information for prostate cancer risk assessment [40]. Robust volume estimation from MRI is needed to help increase clinical use of total and zonal prostate volume information.

The correlation between Gleason score and the TZ volume has not been thoroughly investigated. Ohigashi et al. [39] compared the total prostate and the TZ volume of patients with aggressive (Gleason score, ≥ 7; volume, ≥ 0.5 mL) versus indolent (Gleason score, < 7) cancer and found significantly smaller TZ volume but similar total prostate volume in patients with aggressive prostate cancer. In our study, in addition to central gland volume, we have also investigated the central gland volume fraction as a novel risk factor for significant prostate cancer (Gleason score, ≥ 7). The correlation between Gleason score and the central gland volume fraction was, unfortunately, only modest, thus limiting the clinical utilization of it alone; however, together with other risk factors, this MRI-derived central gland volume fraction could be used to help predict personalized risk of significant prostate cancer, thereby increasing the efficiency of prostate cancer screening and improving patient selection for active surveillance and its outcome.

PSA is the best serum marker for prostate cancer screening, but its discriminating power is limited because of low specificity [41]. On the basis of a review of available scientific evidence, the U.S. Preventive Services Task Force [42] recently concluded that PSA-based screening results in a small or no reduction in prostate cancer–specific mortality and is associated with harms related to subsequent evaluation and treatments. Because of these limitations, a variety of PSA-related serum markers (e.g., volume-adjusted PSA and PSA kinetics) have been investigated. Kalish et al. [32] introduced the concept of PSA adjusted by the TZ volume and concluded that it is more accurate than PSAD in predicting prostate cancer. Since then, many studies have confirmed that adjusting PSA for the total or TZ prostate volumes improves specificity for prostate cancer detection and reduces the number of biopsies [36, 37, 40, 43]. In a recent study of 129 patients who underwent prostatectomy, Ohigashi et al. [39] found that PSA adjusted by the TZ volume (estimated from transrectal ultrasound) was significantly different between patients with indolent versus aggressive prostate cancer. These results are in agreement with the significant correlation that we found between Gleason score and MRI-derived PSAD of the central gland. MRI has the potential to provide robust total and zonal prostate volume measurements, and PSA adjusted by MRI-derived prostate volumes has the potential to facilitate clinical use of PSAD of the central gland for predicting significant prostate cancer.

Our study has several limitations because of its small sample size and retrospective design. Only patients with known prostate cancer were included in our study; therefore, we were not able to evaluate the correlation between the volume parameters and prostate cancer risk. Also, because of the limitations of MRI, we were not able to estimate the TZ volume separately from the central zone. However, in older men such as those included in our study,

the TZ enlarges and the central zone decreases in size, causing most of the central gland to be composed of the TZ [44]. Another limitation of our study is a lack of MRI-based tumor volume– adjusted PSA calculation and evaluation of its performance in predicting aggressive prostate cancer diagnosis. Unfortunately, we were not able to perform precise MRI-histopathology correlation to allow accurate tumor mapping on MRI examinations; however, further investigation of this parameter in future studies will be very helpful.

In conclusion, we found a statistically significant negative correlation between Gleason score and estimates of central gland volume fraction, PSAD, and PSAD of the central gland, on the basis of T2-weighted MRI examinations and semiautomated segmentation software. Although similar parameters based on transrectal ultrasound have been tested previously, MRI may have advantages over transrectal ultrasound and may produce more-accurate delineation of the prostate zonal structure. MRI-based volume parameters have the potential to contribute to personalized risk assessment of significant prostate cancer and warrant further study of their clinical utility.

References

1. D'Amico AV, Whittington R, Malkowicz SB, et al. Biochemical outcome after radical prostatectomy, external beam radiation therapy, or interstitial radiation therapy for clinically localized prostate cancer. JAMA. 1998; 280:969–974. [PubMed: 9749478]
2. Partin AW, Mangold LA, Lamm DM, Walsh PC, Epstein JI, Pearson JD. Contemporary update of prostate cancer staging nomograms (Partin Tables) for the new millennium. Urology. 2001; 58:843–848. [PubMed: 11744442]
3. D'Amico AV, Moul J, Carroll PR, Sun L, Lubeck D, Chen MH. Cancer-specific mortality after surgery or radiation for patients with clinically localized prostate cancer managed during the prostate-specific antigen era. J Clin Oncol. 2003; 21:2163–2172. [PubMed: 12775742]
4. Stephenson AJ, Scardino PT, Eastham JA, et al. Preoperative nomogram predicting the 10-year probability of prostate cancer recurrence after radical prostatectomy. J Natl Cancer Inst. 2006; 98:715–717. [PubMed: 16705126]
5. Bill-Axelson A, Holmberg L, Ruutu M, et al. Radical prostatectomy versus watchful waiting in early prostate cancer. N Engl J Med. 2005; 352:1977–1984. [PubMed: 15888698]
6. Daskivich TJ, Chamie K, Kwan L, et al. Overtreatment of men with low-risk prostate cancer and significant comorbidity. Cancer. 2011; 117:2058–2066. [PubMed: 21523717]
7. Welch HG, Albertsen PC. Prostate cancer diagnosis and treatment after the introduction of prostate-specific antigen screening: 1986–2005. J Natl Cancer Inst. 2009; 101:1325–1329. [PubMed: 19720969]
8. McNeal JE. Regional morphology and pathology of the prostate. Am J Clin Pathol. 1968; 49:347–357. [PubMed: 5645095]
9. Augustin H, Erbersdobler A, Hammerer PG, Graefen M, Huland H. Prostate cancers in the transition zone. Part 2. Clinical aspects. BJU Int. 2004; 94:1226–1229. [PubMed: 15610094]
10. Stamey TA, Dietrick DD, Issa MM. Large, organ confined, impalpable transition zone prostate cancer: association with metastatic levels of prostate specific antigen. J Urol. 1993; 149:510–515. [PubMed: 7679754]
11. Noguchi M, Stamey TA, Neal JE, Yemoto CE. An analysis of 148 consecutive transition zone cancers: clinical and histological characteristics. J Urol. 2000; 163:1751–1755. [PubMed: 10799175]
12. Augustin H, Erbersdobler A, Graefen M, et al. Biochemical recurrence following radical prostatectomy: a comparison between prostate cancers located in different anatomical zones. Prostate. 2003; 55:48–54. [PubMed: 12640660]

13. Lee F, Siders DB, Torp-Pedersen ST, Kirscht JL, McHugh TA, Mitchell AE. Prostate cancer: transrectal ultrasound and pathology comparison: a preliminary study of outer gland (peripheral and central zones) and inner gland (transition zone) cancer. Cancer. 1991; 67(suppl):1132–1142. [PubMed: 1991271]
14. Ishida J, Sugimura K, Okizuka H, et al. Benign prostatic hyperplasia: value of MR imaging for determining histologic type. Radiology. 1994; 190:329–331. [PubMed: 7506836]
15. Kahn T, Bürrig K, Schmitz-Dräger B, Lewin JS, Fürst G, Mödder U. Prostatic carcinoma and benign prostatic hyperplasia: MR imaging with histopathologic correlation. Radiology. 1989; 173:847–851. [PubMed: 2479050]
16. Schiebler ML, Tomaszewski JE, Bezzi M, et al. Prostatic carcinoma and benign prostatic hyperpla sia: correlation of high-resolution MR and histopathologic findings. Radiology. 1989; 172:131–137. [PubMed: 2472644]
17. Hricak H, Dooms GC, McNeal JE, et al. MR imaging of the prostate gland: normal anatomy. AJR. 1987; 148:51–58. [PubMed: 3491523]
18. Sommer FG, McNeal JE, Carrol CL. MR depiction of zonal anatomy of the prostate at 1.5 T. J Comput Assist Tomogr. 1986; 10:983–989. [PubMed: 3782570]
19. Oto A, Kayhan A, Jiang Y, et al. Prostate cancer: differentiation of central gland cancer from benign prostatic hyperplasia by using diffusion-weighted and dynamic contrast-enhanced MR imaging. Radiology. 2010; 257:715–723. [PubMed: 20843992]
20. Lee JS, Chung BH. Transrectal ultrasound versus magnetic resonance imaging in the estimation of prostate volume as compared with radical prostatectomy specimens. Urol Int. 2007; 78:323–327. [PubMed: 17495490]
21. Jeong CW, Park HK, Hong SK, Byun SS, Lee HJ, Lee SE. Comparison of prostate volume measured by transrectal ultrasonography and MRI with the actual prostate volume measured after radical prostatectomy. Urol Int. 2008; 81:179–185. [PubMed: 18758216]
22. Milosevic M, Voruganti S, Blend R, et al. Magnetic resonance imaging (MRI) for localization of the prostatic apex: comparison to computed tomography (CT) and urethrography. Radiother Oncol. 1998; 47:277–284. [PubMed: 9681891]
23. Choi YJ, Kim JK, Kim HJ, Cho KS. Interobserver variability of transrectal ultrasound for prostate volume measurement according to volume and observer experience. AJR. 2009; 192:444–449. [PubMed: 19155408]
24. Jia G, Baudendistel KT, von Tengg-Kobligk H, et al. Assessing prostate volume by magnetic resonance imaging: a comparison of different measurement approaches for organ volume analysis. Invest Radiol. 2005; 40:243–248. [PubMed: 15770143]
25. Bulman JC, Toth R, Patel AD, et al. Automated computer-derived prostate volumes from MR imaging data: comparison with radiologist-derived MR imaging and pathologic specimen volumes. Radiology. 2012; 262:144–151. [PubMed: 22190657]
26. Liao S, Gao Y, Shen D. Sparse patch based prostate segmentation in CT images. Med Image Comput Comput Assist Interv. 2012; 15:385–392. [PubMed: 23286154]
27. Rodriguez E Jr, Skarecky D, Narula N, Ahlering TE. Prostate volume estimation using the ellipsoid formula consistently underestimates actual gland size. J Urol. 2008; 179:501–503. [PubMed: 18076916]
28. Varma M, Morgan JM. The weight of the prostate gland is an excellent surrogate for gland volume. Histopathology. 2010; 57:55–58. [PubMed: 20653780]
29. Ohlsén H, Ekman P, Ringertz H. Assessment of prostatic size with computed tomography: methodologic aspects. Acta Radiol Diagn (Stockh). 1982; 23(3A):219–223. [PubMed: 6181654]
30. Metz CE, Pan X. “Proper” binormal ROC curves: theory and maximum-likelihood estimation. J Math Psychol. 1999; 43:1–33. [PubMed: 10069933]
31. Kaplan SA, Te AE, Pressler LB, Olsson CA. Transition zone index as a method of assessing benign prostatic hyperplasia: correlation with symptoms, urine flow and detrusor pressure. J Urol. 1995; 154:1764–1769. [PubMed: 7563342]
32. Kalish J, Cooner WH, Graham SD Jr. Serum PSA adjusted for volume of transition zone (PSAT) is more accurate than PSA adjusted for total gland volume (PSAD) in detecting adenocarcinoma of the prostate. Urology. 1994; 43:601–606. [PubMed: 7513104]

33. Tewari A, Shinohara K, Narayan P. Transition zone volume and transition zone ratio: predictor of uroflow response to finasteride therapy in benign prostatic hyperplasia patients. Urology. 1995; 45:258–264. [PubMed: 7531900]
34. Djavan B, Zlotta AR, Byttebier G, et al. Prostate specific antigen density of the transition zone for early detection of prostate cancer. J Urol. 1998; 160:411–418. [PubMed: 9679889]
35. Djavan B, Remzi M, Zlotta AR, et al. Complexed prostate-specific antigen, complexed prostate-specific antigen density of total and transition zone, complexed/total prostate-specific antigen ratio, free-to-total prostate-specific antigen ratio, density of total and transition zone prostate-specific antigen: results of the prospective multicenter European trial. Urology. 2002; 60(suppl 1): 4–9. [PubMed: 12384156]
36. Kang SH, Bae JH, Park HS, et al. Prostate-specific antigen adjusted for the transition zone volume as a second screening test: a prospective study of 248 cases. Int J Urol. 2006; 13:910–914. [PubMed: 16882054]
37. Zlotta AR, Djavan B, Petein M, Susani M, Marberger M, Schulman CC. Prostate specific antigen density of the transition zone for predicting pathological stage of localized prostate cancer in patients with serum prostate specific antigen less than 10 ng/ml. J Urol. 1998; 160:2089–2095. [PubMed: 9817330]
38. Ohi M, Ito K, Suzuki K, Yamamoto T, Yamanaka H. Diagnostic significance of PSA density adjusted by transition zone volume in males with PSA levels between 2 and 4 ng/ml. Eur Urol. 2004; 45:92–96. [PubMed: 14667523]
39. Ohigashi T, Kanao K, Mizuno R, Kikuchi E, Nakashima J, Oya M. Predicting the probability of significant prostate cancer in Japanese men with serum prostate-specific antigen less than 10 ng/mL: development of a novel pre-biopsy nomogram. Int J Urol. 2010; 17:274–280. [PubMed: 20148990]
40. Tanaka N, Fujimoto K, Chihara Y, et al. Prostatic volume and volume-adjusted prostate-specific antigen as predictive parameters for prostate cancer patients with intermediate PSA levels. Prostate Cancer Prostatic Dis. 2007; 10:274–278. [PubMed: 17339878]
41. Catalona WJ, Richie JP, Ahmann FR, et al. Comparison of digital rectal examination and serum prostate specific antigen in the early detection of prostate cancer: result of a multicenter trial of 6,630 men. J Urol. 1994; 151:1283–1290. [PubMed: 7512659]
42. Lin, K.; Croswell, JM.; Koenig, H.; Lam, C.; Maltz, A. Prostate-specific antigen-based screening for prostate cancer: an evidence update for the U.S. Preventive Services Task Force—evidence synthesis no. 90. AHRQ Publication No. 12-05160-EF-1. Rockville, MD: Agency for Healthcare Research and Quality; 2011.
43. Benson MC, Whang IS, Olsson CA, McMahon DJ, Cooner WH. The use of prostate specific antigen density to enhance the predictive value of intermediate levels of serum prostate specific antigen. J Urol. 1992; 147:817–821. [PubMed: 1371555]
44. McNeal JE. The prostate gland: morphology and pathobiology. Monogr Urol. 1983; 4:5–13.

APPENDIX 1: MRI Acquisition Protocols

For the Excite (GE Healthcare) unit protocol, an array spatial sensitivity encoding technique (parallel imaging) factor of 2 was used in all sequences. T2-weighted imaging parameters were as follows: TR/TE, 3200–3500/90–100; matrix, 192 × 256; echo-train length, 19; number of signals acquired, 4; section thickness, 3 mm; intersection gap, 0 mm; and FOV, 14–16 cm. Diffusion-weighted imaging parameters were as follows: TR/TE, 7000–8000/80–90; matrix, 128 × 128–224; b value = 0, 1000, and 1500 s/mm^2; section thickness, 4 mm; gap, 0 mm; number of signals acquired, 4; and FOV, 14– 18 cm. T1-weighted 3D gradient-echo free-breathing axial dynamic contrast-enhanced MRI examinations covering the entire prostate were acquired starting 30 seconds before the IV administration of gadodiamide at a dose of 0.1 mmol/kg, followed by a 20-mL saline flush at a rate of 2.0 mL/s. Dynamic contrast-enhanced MRI parameters were as follows: TR/TE, 3.5–3.9/1.6–1.9; matrix, 160 ×

256; flip angle, 10°; and interpolated section thickness, 3 mm with a temporal resolution of 5–12 seconds for approximately 5–7 minutes. Approximately 30–50 sets of images were acquired to monitor the time course of contrast agent uptake and clearance within the prostate. The entire imaging protocol, including patient preparation, was performed in less than 1 hour for all patients.

For the Achieva (Philips Healthcare) unit protocol, an effective sensitivity encoding (parallel imaging) factor of 2 was used in all sequences. T2-weighted imaging parameters were as follows: spatial resolution, 0.8 × 0.8 × 3 mm; TR/TE, 4300–5000/120; matrix, 204 × 256; echo-train length, 24; number of signals acquired, 4; section thickness, 3 mm; intersection gap, 0 mm; and FOV, 1418 cm. Diffusion-weighted imaging parameters were as follows: TR/TE, 3800–4200/80–90; matrix, 128 × 128; b value = 0, 1000, and 1500 s/mm^2; section thickness, 4 mm; gap, 0 mm; number of signals acquired, 4; and FOV, 14–18 cm. Dynamic contrast-enhanced MRI parameters were as follows: 3D fast-field-echo; TR/TE, 5.5/2.1; matrix, 199 × 292; and interpolated section thickness, 3 mm with a temporal resolution of 3–5 seconds for approximately 7–9 minutes. The dose and administration of IV gadolinium was similar to those in the GE Healthcare unit protocol. Approximately 70–100 sets of images were acquired, and the entire imaging protocol, including patient preparation, was performed in less than 1 hour for all patients.

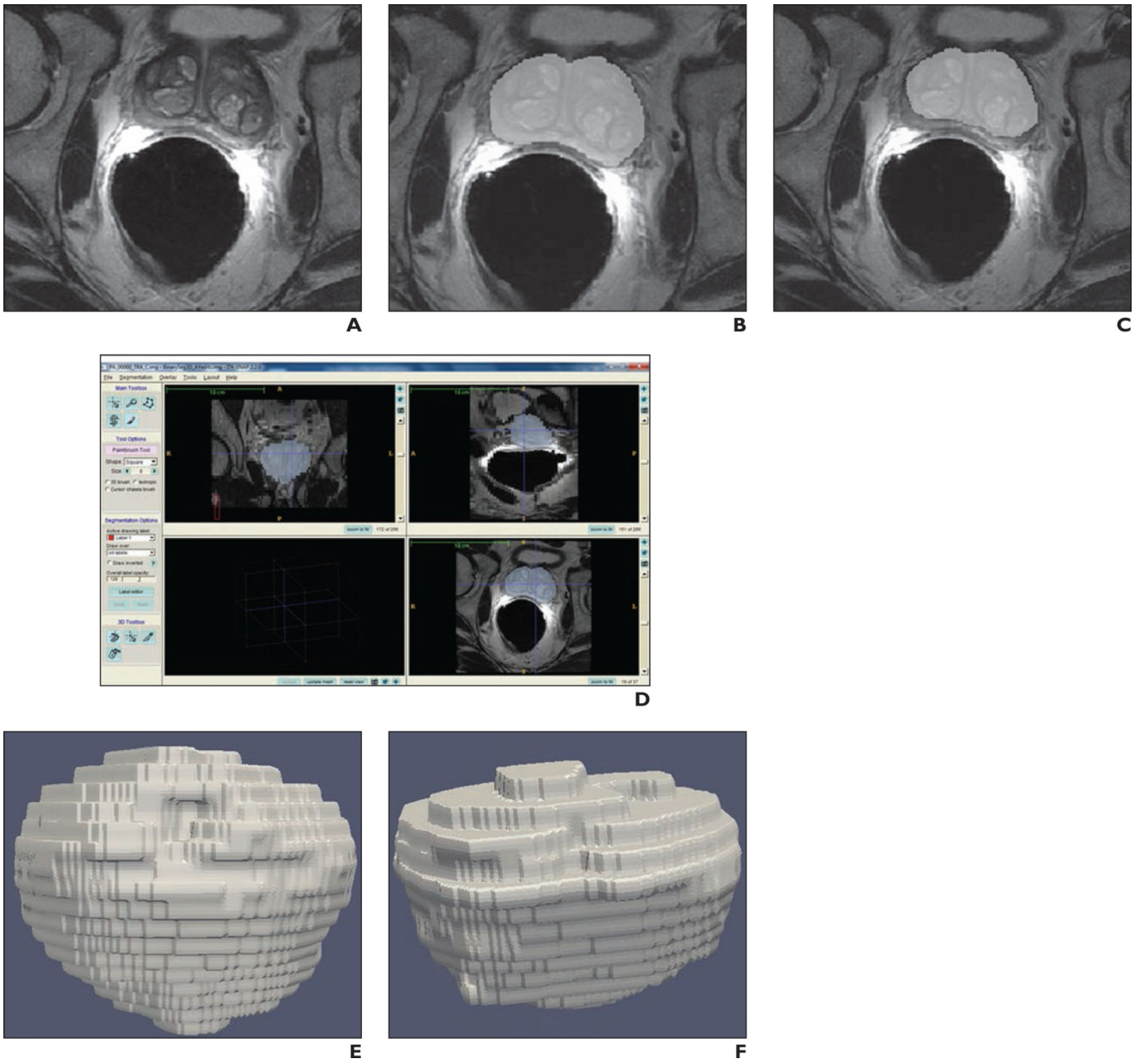

Fig. 1.

66-year-old man who underwent prostatectomy for prostate cancer (Gleason score of 6 = 3 + 3; prostate-specific antigen level, 7.09 ng/mL).

A, Axial T2-weighted fast spin-echo MRI was obtained through mid prostate without labeling of segmentation results.

B, Labeled segmentation result of entire prostate is seen on T2-weighted axial image by using semiautomated segmentation software and ITKSNAP software (Penn Image Computing and Science Laboratory).

C, Labeled segmentation result of central gland is shown.

D, Screen-capture display from adapted ITKsnap software shows simultaneous display of axial, coronal, and sagittal images during manual correction of segmentation results.

E, Entire prostate is seen on 3D volume image.

F, Central gland is seen on 3D volume image. Total prostate weight was 52.7 g, estimated prostate volume was 46.25 cm^3, and estimated central gland volume was 30.57 cm^3.

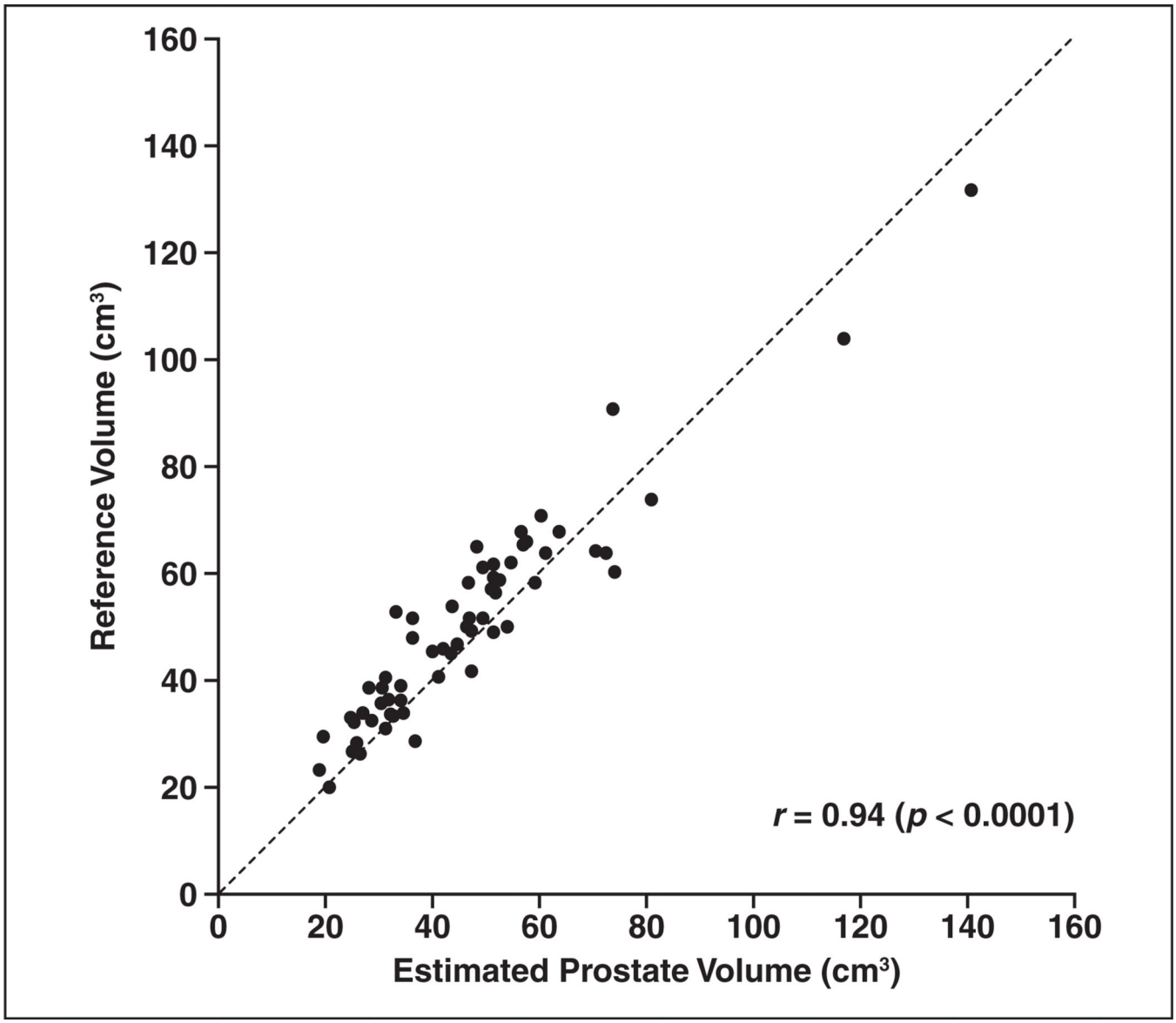

Fig. 2.

Correlation between estimated total prostate volume from MRI examinations and reference standard of prostate volume based on prostatectomy specimen weight. Also shown are Pearson correlation coefficient (*r*) and its *p* value and identity line (*dashed line*).

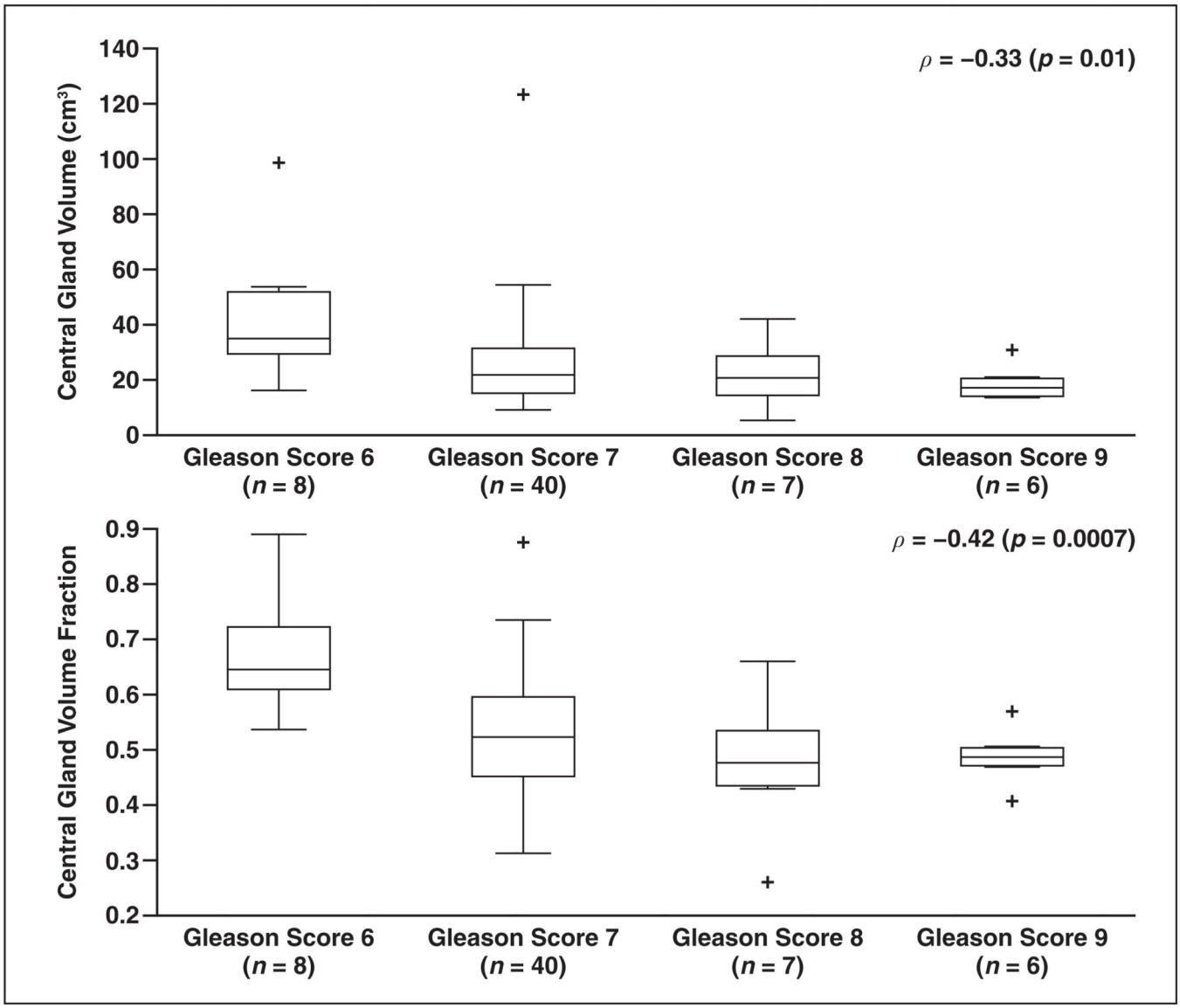

Fig. 3.

Box-and-whisker plots of correlation between Gleason score and estimated central gland volume (*top*) and between Gleason score and central gland volume fraction (*bottom*). Lines denote medians, boxes denote first and third quartiles, and data points beyond whiskers are considered as outliers. Also shown are Spearman correlation coefficients (ρ) and their *p* values.

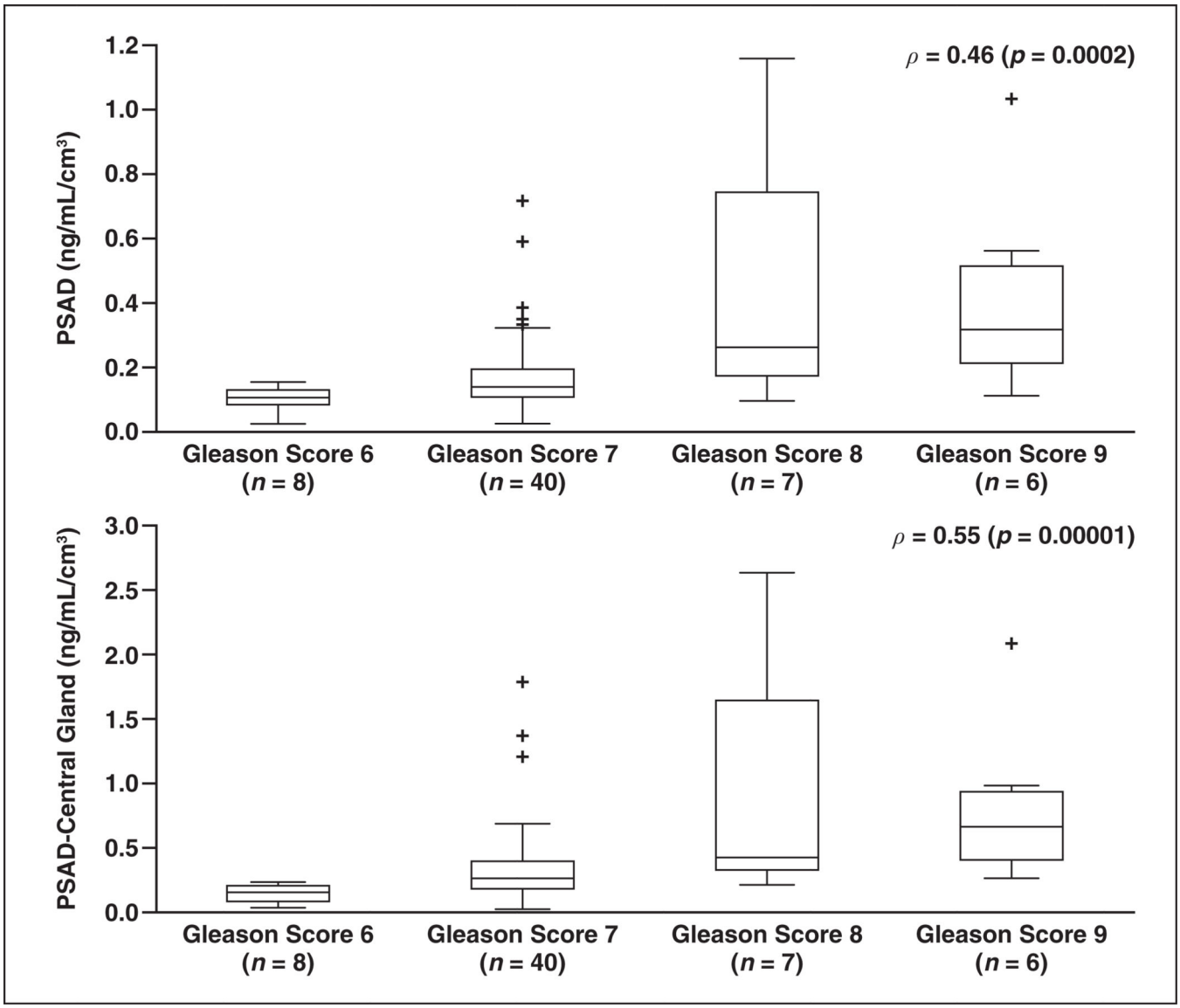

Fig. 4.

Box-and-whisker plots of correlation between Gleason score and prostate-specific antigen density (PSAD) (*top*) and between Gleason score and central gland volume–adjusted prostate-specific antigen (PSAD of central gland) (*bottom*). Lines denote medians, boxes denote first and third quartiles, and data points beyond whiskers are considered as outliers. Also shown are Spearman correlation coefficients (ρ) and their *p* values.

TABLE 1

Estimated Peripheral Zone, Central Gland, and Total Prostate Volumes in 61 Patients According to MRI

Location	Mean (cm^3)	Median (cm^3)	SD (cm^3)	Range (cm^3)
Peripheral zone	19.5	18.6	6.1	6.6–32.6
Central gland	26.9	21.6	19.3	5.1–123.4
Total prostate	46.4	44.5	21.2	18.7–140.7

TABLE 2

Spearman Correlation Coefficients Between Gleason Score and Age, Estimated Total, Peripheral Zone (PZ), and Central Gland Prostate Volumes and Estimated Central Gland Volume Fraction, Prostate-Specific Antigen (PSA), and PSA Densities (PSADs)

		Volume				PSAD			
Statistical Comparison	**Age**	**Prostate**	**PZ**	**Central Gland**	**Central Gland Volume Fraction**	**PSAD**	**PSAD of Central Gland**	**PSAD of PZ**	**PSA**
Correlation coefficient	0.04	−0.16	0.06	−0.33	**−0.42**	**0.46**	**0.55**	0.26	0.29
p	0.78	0.11	0.65	0.01[a,b]	0.0007[a]	0.0002[a]	0.00001[a]	0.04[a,b]	0.03[a,b]

[a]Denotes statistically significant *p* values; corresponding correlation coefficients are shown in **bold type**.

[b]Fails to show statistical significance after Bonferroni correction ($p > 0.005$).

TABLE 3

Effectiveness of MRI Volume-Derived Parameters for Differentiation Between Prostate Cancers With Gleason Score < 7 and ≥ 7

Parameter	Sensitivity	Specificity	PPV	NPV	Threshold
Central gland volume fraction[a]	83 (44/53)	75 (6/8)	96 (44/46)	40 (6/15)	0.62
PSAD[b]	79 (42/53)	63 (5/8)	93 (42/45)	31 (5/16)	0.11[c]
PSAD of central gland[b]	85 (45/53)	63 (5/8)	94 (45/48)	38 (5/13)	0.16[c]

Note—Data are percentage (no./total). The threshold values were selected empirically on the basis of this patient dataset. NPV = negative predictive value, PPV = positive predictive value.

[a] A smaller value indicates that cancer is more likely to have a Gleason score ≥ 7.

[b] A larger value indicates that cancer is more likely to have a Gleason score ≥ 7.

[c] Unit of measurement is ng/mL/cm^3.